

Investigation of welding parameter dependent microstructure and mechanical properties in friction stir welded pure Ti joints

Hidetoshi Fujii*, Yufeng Sun, Hideaki Kato, Kazuhiro Nakata

Joining and Welding Research Institute, Osaka University, 11-1 Mihogaoka, Ibaraki 567-0047, Japan

ARTICLE INFO

Article history:

Received 24 November 2009

Received in revised form 19 January 2010

Accepted 8 February 2010

Keywords:

Friction stir welding
Mechanical properties
Dynamic recrystallization
Hall–Petch relation

ABSTRACT

Commercial purity titanium plates with 2 mm in thickness were successfully friction stir butt-welded at a welding speed ranged from 50 to 300 mm/min. The measured peak temperatures during all the welding processes were below the α/β phase transformation point. The microstructural characterization revealed that the stir zone has an equiaxial grain structure and low density of dislocations at lower welding speed, but a high density of dislocations at higher welding speed. The optimized tensile property was obtained for the specimen welded at 200 mm/min. The mechanical properties related to the microstructural evolution were investigated and discussed by comparing with the Al (fcc) and IF steel (bcc) results.

© 2010 Elsevier B.V. All rights reserved.

1. Introduction

Titanium and titanium alloys have been widely used in the aerospace industry due to their high specific strength, high heat resistant and high corrosion resistant properties. Recently, titanium alloys have also been explored as potential biomedical materials because of their low allergy risk to the human bodies. When used as structural materials, titanium and titanium alloys have been generally regarded as weldable by fusion welding methods like arc welding, laser welding, etc. However, distortion of the fusion welded materials usually takes place due to the low thermal conductivity of titanium. Moreover, the titanium and titanium alloys are highly reactive in the molten state and the formation of titanium oxide and porosities in the weld nuggets will inevitably results in the degradation of the mechanical properties. Since the invention of the friction stir welding (FSW) technique by TWI in 1991, the FSW of low melting point materials such as Al [1–4], Mg [5–6], and Cu [7] have been widely investigated. Recently, the studies on the friction stir weldability of widely used high melting point materials, such as cast iron [8], carbon steel [9–12], and stainless steel [13–16], have also started. However, there are only a few reports concerning the FSW of titanium or titanium alloys [17,18,20]. Comparing with steel materials, the melting point of titanium is higher and durable tools at high temperature are strongly required. In addition, titanium possesses a stable hcp structure at ambient temperature and will transform to a bcc structure when the temperature

is higher than 880 °C. The allotropic phase transformation might occur during the continuous deformation, heating and cooling process when the FSW is performed, which makes it more difficult to obtain sound joints. With the development of rotation tools, nowadays titanium or titanium alloys can be successfully FSW processed using high temperature durable tools like coated TiC tools and WC alloys tools, etc. For example, Lee et al. [17] and Ramirez and Juhas [18] succeeded in producing pure Ti joints and Ti–6Al–4V joints, respectively. John et al. [19] investigated the residual stress of FSW processed Ti–6Al–4V and more recently Mironov et al. [21,22] reported detailedly the texture evolution in the FSW of Ti and Ti–6Al–4V alloys. These interesting studies indicated that improved mechanical properties of the joint of titanium or titanium alloys can be accomplished by using the FSW technique. However, the effect of the welding conditions on the microstructure and mechanical properties has not been thoroughly studied.

In this study, 2 mm thick commercial pure titanium (cp-Ti) plates were successfully friction stir welded at a temperature lower than the α/β phase transformation point. The optimized welding parameter was determined by comparing the mechanical properties of the joints obtained under different welding conditions. Also, the differences in the mechanical properties and microstructure were investigated and discussed by comparing with Al (fcc) and steel (bcc) results.

2. Experimental procedures

Cp-Ti plates with dimension of $300^l \times 50^w \times 2^t$ mm³ were butt-welded by the FSW technique under the load-control mode. The chemical composition of the cp-Ti is 0.007C–0.0013B–0.080–

* Corresponding author. Tel.: +81 6 68798663; fax: +81 6 68798663.
E-mail address: fujii@jwri.osaka-u.ac.jp (H. Fujii).

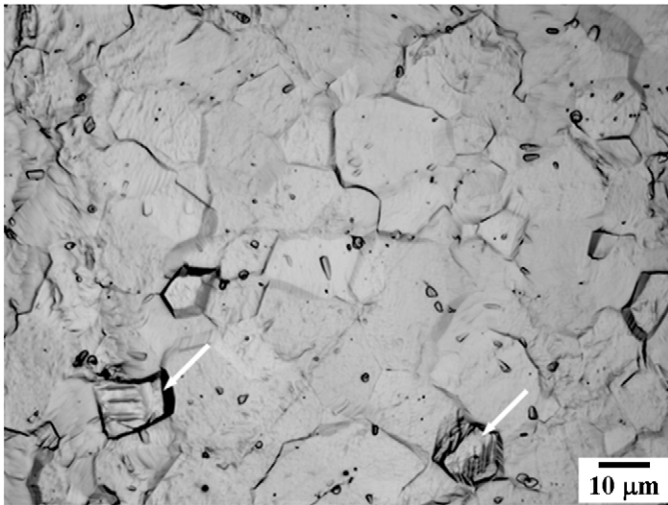


Fig. 1. OM showing the microstructure of the as-received cp-Ti plate.

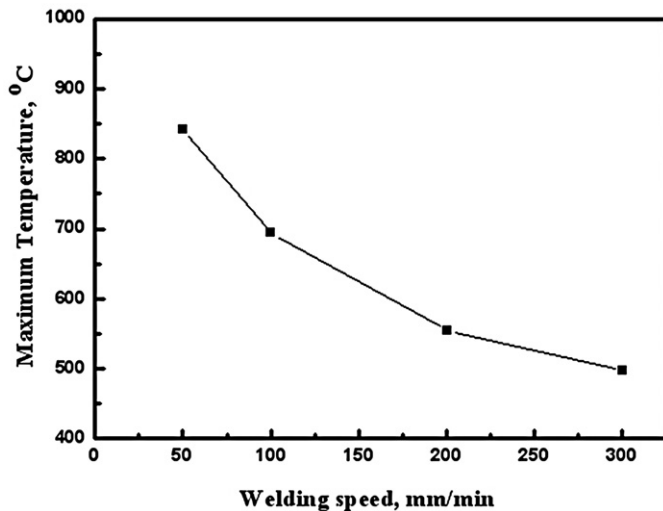


Fig. 2. Peak temperature measured in the stir zone welded at different welding speeds.

0.004N–0.05Fe (in wt.%). Tungsten carbide based alloy tools whose shoulder diameter was 15 mm, probe diameter was 6 mm and probe length was 1.8 mm, were used for all the welding processes. The tool rotation speed was fixed at 200 rpm and the welding speed was varied within the range from 50 to 300 mm/min. During welding, a protective atmosphere of Ar gas flowed around the tool to prevent the joints from being oxidized and the temperature rise was measured by thermocouples placed under the bottom of the cp-Ti plates. The microstructure in the stir zone was observed by optical microscopy (OM), electronic backscattering diffraction (EBSD) and transmission electron microscopy (TEM). The dog bone-like tensile specimens were cut by an electrical discharge machine perpendicular to the welding direction and the tensile tests were carried out at a cross-head speed of 1 mm/min. The Vickers microhardness distribution was measured under a load of 0.98 N for a dwell time of 15 s along the centerlines of the cross-section with an interval of 0.5 mm.

3. Experimental results

Fig. 1 shows the OM images of the microstructure of the as-received cp-Ti plate, which has an equiaxed grain structure with

an average grain size of about 10 μm . A lamellar twin structure can be found within some grains, which is indicated by the white arrows in the figure.

Fig. 2 shows the measured peak temperature in the stir zone of the cp-Ti welds processed at different welding speeds. It revealed that the maximum temperature during the welding process can reach 843, 694, 555 and 498 $^{\circ}\text{C}$ at a welding speed of 50, 100, 200 and 300 mm/min, respectively. This means that all the FSW of cp-Ti was processed below the α/β phase transformation temperature, despite of the welding speeds used in the present study. In addition, the work-pieces were exposed at high temperature for a very short time due to the rapid moving of the rotating tools. Therefore, it is believed that no phase transformation occurred under all these welding conditions.

Fig. 3 shows the EBSD maps and the corresponding $\{0001\}$ pore figures for the stir zone obtained at a welding speed of 50, 100, 200 and 300 mm/min. Fig. 3(a) briefly illustrates the locations where the EBSD measurements were carried out. The measured points with a confidence index (CI) value less than 0.05 were blacked out in the EBSD maps and removed from the calculation of the pore figures. Generally, the stir zones all exhibit an equiaxial grain structure regardless of the welding speeds, indicating the occurrence of dynamic recrystallization during the welding process. In addition, the average grain size decreased with the increasing welding speed due to the less heat input. In the stir zone welded at 50 mm/min as shown in Fig. 3(b), some grains with a remarkably larger size can be distinguished and are indicated by the white arrows, which should be the secondary recrystallized grains due to the relatively higher heat input during the welding process. The secondary recrystallized grains all exhibit a red color indicating their $[0001]$ axes parallel with the ND. From the corresponding $\{0001\}$ pore figures, it was found that a strong crystallographic texture formed in the stir zone and significantly depended on the welding speed. For the sample welded at 50 mm/min, the texture intensity can achieve about 34.4 times random. However, the texture intensity decreased to 32.2, 25.0 and 15.3 times random when the welding speed increased to 100, 200 and 300 mm/min respectively. This is quite different with the other FSW processed materials like Al, Cu or Mg that the stir zone usually exhibits a random grain orientation. Recently, the strong texture formation in the FSW processed pure titanium was studied in detail by Minorov et al. [22], who pointed out that the grain structure evolution in the stir zone was mainly driven by the texture-induced grain convergence.

The microstructures at the center of the stir zones were further investigated by TEM observations and the typical TEM images of the stir zone welded at 50, 100, 200 and 300 mm/min are shown in Fig. 4(a)–(d). All the stir zones showed an equiaxed grain structure and the average grain size significantly decreased with the increase of welding speed due to the reduced heat input. In addition, the dislocation densities inside the equiaxed grains increase with increasing the welding speed. In Fig. 4(c) and (d), some dislocation tangles can be observed, implying the incomplete or continuous recovery of the cp-Ti.

For comparison purposes, the typical TEM images of the microstructure of the FSW processed pure Al, IF steel and cp-Ti are presented in Fig. 5(a)–(c), respectively. The FSW process of Al and IF steel were carried out at a rotation speed of 400 rpm and a traveling speed of 1000 mm/min, which also indicates a low heat input during the welding for the specific materials. Compared with FSW processed cp-Ti that dislocations of high density distributed inside the grains, there are few dislocation that can be observed in the Al and IF steel joints. This is because of the easy dislocation annihilation due to the high stacking fault energy of pure Al and the bcc crystalline structure of IF steel.

Fig. 6 shows the Vickers microhardness distributed along the centerlines on the cross-sections of the stir zone, in which the bro-

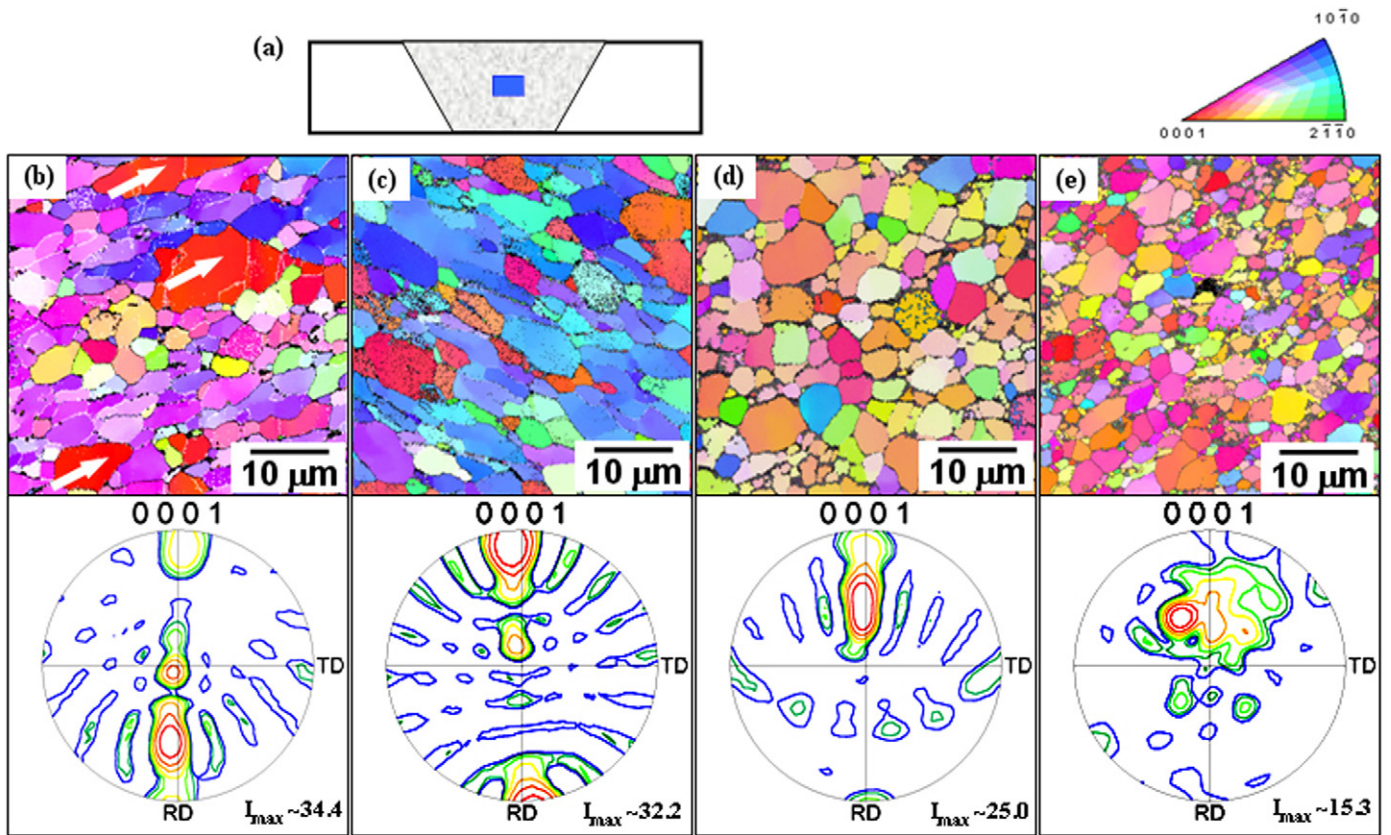


Fig. 3. (a) Schematic diagram showing the locations where the EBSD map was measured; and EBSD map of the stir zone welded at different welding speed of (b) 50 mm/min; (c) 100 mm/min; (d) 200 mm/min and (e) 300 mm/min.

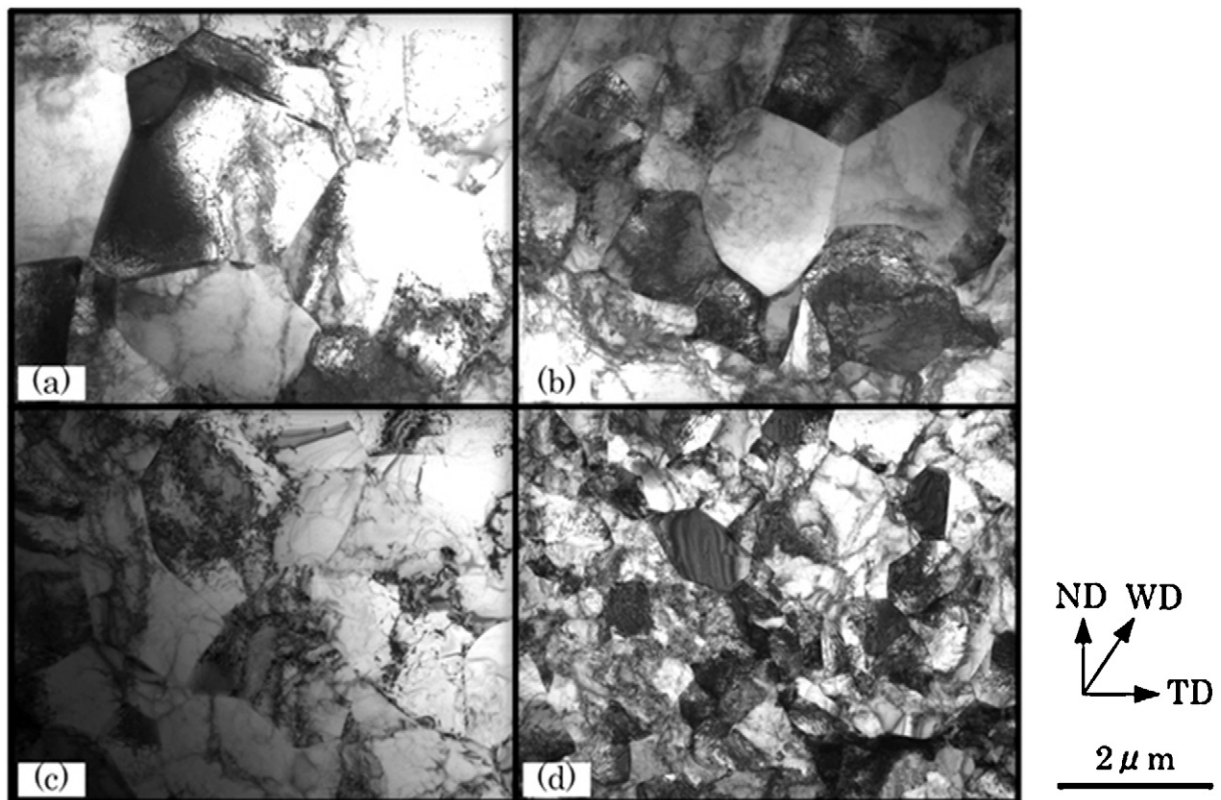


Fig. 4. TEM images showing the microstructure of the stir zone at welding speed of (a) 50 mm/min; (b) 100 mm/min; (c) 200 mm/min; and (d) 300 mm/min.

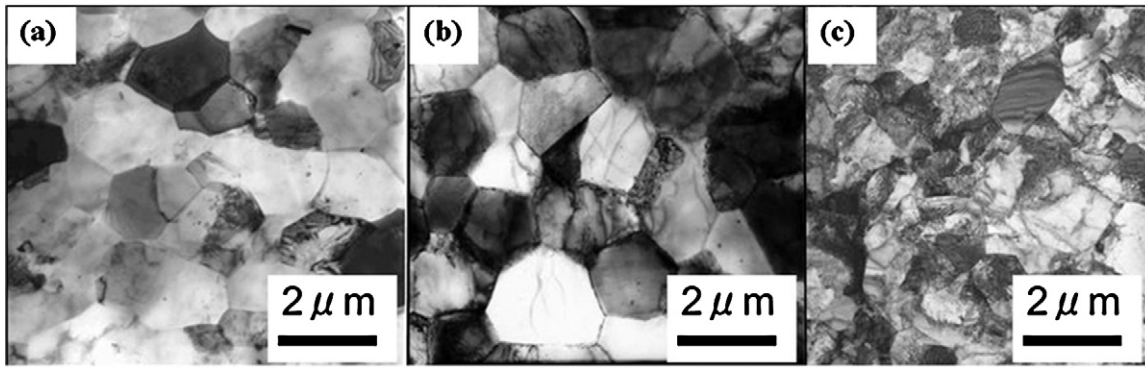


Fig. 5. TEM images showing the microstructure of FSW processed (a) Al; (b) IF Steel; and (c) cp-Ti.

ken line indicates the hardness of the base metal. It can be found that the hardness in the stir zone increases with increasing welding speed. For example, the hardness increased from 150 HV in the stir zone welded at 50 mm/min to about 190 HV in that welded at 300 mm/min.

Fig. 7 shows the tensile strength of the FSW of cp-Ti processed at different welding speeds. The tensile strength of the base metals is about 420 MPa and was also plotted with a dotted line in the figure. For the samples processed at a welding speed smaller than 200 mm/min, the fracture occurred in the stir zone indicating that the strength of the welded sample is less than that of the base metal. However, the tensile strength increases with increasing the welding speed due to the microstructure refinement. When the welding speed increased to 200 mm/min, the tensile strength of the joint exceeded that of the base metal. As a result, the specimen fractured in the base metal during the tensile tests. To evaluate the tensile strength of the welded joint, a miniature tensile specimen was cut in dog bone shape with the gauge length completely within the welded joint. The tensile tests of the miniature specimen showed that the tensile strength of the welded joint is about 450 MPa. However, when the welding speed increased to 300 mm/min, the tensile strength of the specimens decreased again despite the rather significant refinement of the microstructure. The low tensile strength is due to the formation of weld defects in the stir zone caused by the insufficient plastic flow during the welding process. Therefore, the best welding speed for the FSW of cp-Ti is 200 mm/min in the present study.

Table 1

Summary of the grain size and hardness of the samples welded under different conditions.

Welding speed (mm/min)	Grain size (μm)	Hardness (HV)
Base metal	10	146
50	6.3	150
150	4	175
200	3.8	180
300	3.5	190

Table 1 summarizes the average grain size and the Vickers microhardness of the stir zone under various rotation speeds, as well as that of the base metal. The average grain sizes are determined by the linear intercept method based on the OM and EBSD observation. Generally, all the welds have a grain size smaller than the base metal. The average grain size was 6.3, 4, 3.8 and 3.5 μm for the welding speeds of 50, 150, 200 and 300 mm/min, respectively. Compared to the base metal, the FSW resulted in a significant decrease in the grain size in the stir zone due to the occurrence of dynamic recrystallization. Simultaneously, the significant grain refinement resulted from the FSW increased the hardness in the stir zone.

It is well known that for conventional polycrystals with grain size ranging from several to hundreds of micrometers, the hardness dependence on mean grain size can be described by the Hall–Petch relation, $HV = HV_0 + kd^{-1/2}$, Where HV is the hardness of a polycrystalline metal, d is the grain size and HV_0 and k are constants. The

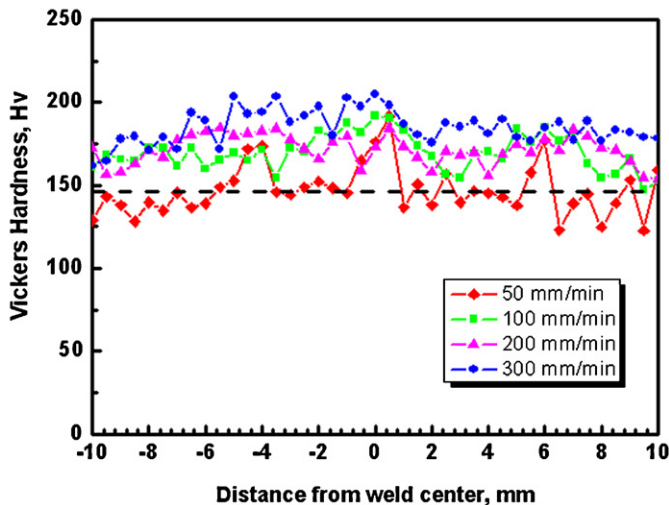


Fig. 6. Hardness profile in the stir zone welded at 50, 100, 200 and 300 mm/min, together with the hardness of the base metals.

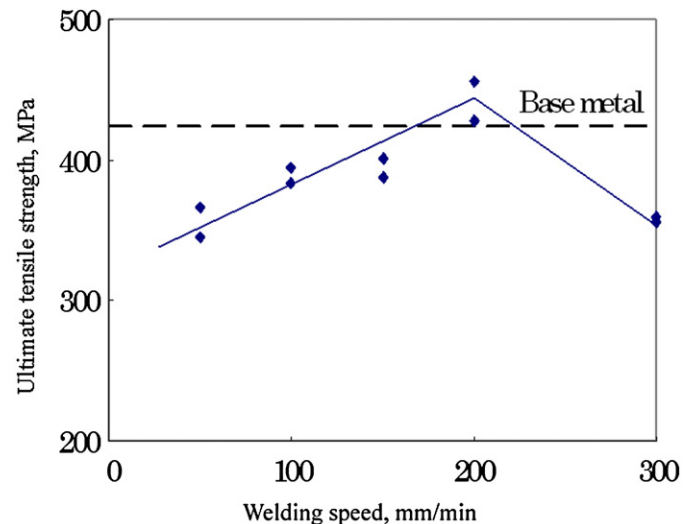


Fig. 7. Tensile strength of the samples at different welding speeds, together with that of the base metal.

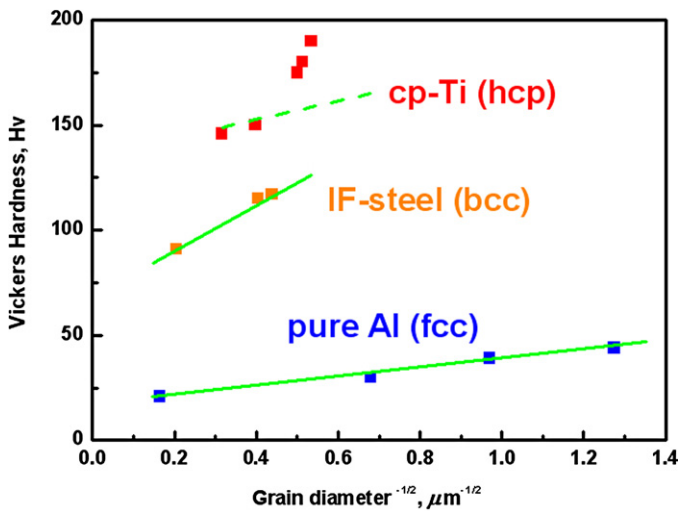


Fig. 8. The hardness and grain size relationship of the FSW processed cp-Ti.

Hall–Petch relation predicts an increased hardness with a decrease in the grain size. Fig. 8 shows the hardness vs. grain size relationship of the FSW processed cp-Ti. For the purpose of comparison, the hardness vs. grain size relationship of the FSW processed pure Al and IF steel is also plotted. In this figure the Hall–Petch line for cp-Ti was extrapolated according to ref. [23]. It is found that the hardness data of the pure Al and IF steel fell on the straight lines representing the Hall–Petch relation. However, for cp-Ti, the experimental data matches well with the Hall–Petch line when the grain size is larger than 6.4 μm. However, when the grain size decreased to less than 6.4 μm, the measured hardness data was obviously higher than those predicted by the Hall–Petch relation.

4. Discussion

The above descriptions revealed that the FSW of cp-Ti can be accomplished below the α/β phase transformation temperature. According to the previous publications about the FSW of pure Ti, the temperature rise caused by friction is usually higher than the phase transformation point [17]. As a result, a serrated grain boundary can usually be found in the stir zone due to the $\beta \rightarrow \alpha$ phase transformation during the subsequent cooling after the welding process. However, no such serrated grain boundary was found in the present study. This reveals that the FSW of cp-Ti could be obtained under the phase transformation temperature, which was also confirmed by the instantaneous temperature measurement. The low temperature rise during the FSW process has at least two advantages to obtain a sound welded joint. The low temperature can prevent the rapid growth of the recrystallized grains and therefore improve the mechanical properties of the stir zone. On the other hands, the prevention of the phase transformation will help the smooth proceeding of the FSW process, since the formation of the β phase has a bcc structure and much lower strength than the α phase, which might lead to the sudden sinking of the rotation tools.

It is also noteworthy that the relationship of the hardness and average grain size in the stir zone does not match the Hall–Petch relation within the whole grain size range. Recently, some examples of the deviation of Hall–Petch relation were found in nanostructured metals [24]. However, FSW processed materials have an average grain size seldom less than 1 μm and usually follow the Hall–Petch relation. The deviation of the Hall–Petch relation in this study is probably attributed to the two aspects. First, for the cp-Ti welded at high speed, like 200 or 300 mm/min

(minimum heat input in this study), a significant amount of dislocations are generated in the deformed grains due to the incomplete recovery and dynamic recrystallization at low temperature. The tangling of the high density dislocations will inevitably result in the higher hardness value, compared to the completely recovered grains, i.e., dislocation-free samples. On the other hand, the crystallography texture in the stir zone processed at low welding speeds is much higher than those welded at high welding speed, which means that a large fraction of the grains having a similar orientation, or low misorientations exists in the stir zones processed at lower welding speed. Since the microhardness on the free surface of the polycrystalline metals is closely related to the inhomogeneous deformation in the respective grains, the low misorientation between the neighboring grains cannot effectively block the dislocations moving through the grain boundaries under the external stress and therefore reveals a lower hardness value. Comparing with cp-Ti, there are few dislocations and no obvious crystallography textures in the FSW processed Al or IF steel obtained within a wide welding speed range. The disappearance of the dislocation after the FSW is due to their easy recovery at low temperature. Therefore, the Hall–Petch relation can be successfully applied to the FSW processed Al and IF steel.

5. Conclusions

In this study, the cp-Ti plates with 2 mm in thickness were successfully friction stir butt-welded under different processing conditions. The microstructure and the mechanical properties of the stir zone were investigated. In summary, the following conclusions can be drawn.

- (1) The cp-Ti plates can be friction stir welded at a welding speed from 50 to 300 mm/min and the optimized overall mechanical properties was obtained at a welding speed of 200 mm/min.
- (2) A high crystallography texture of 34.4 times random formed in the stir zone when welded at the low welding speed of 50 mm/min. However, the texture strength decreased with increasing the welding speed and finally decreased to 15.3 times random at the welding speed of 300 mm/min.
- (3) The measured hardness value and the average grain size in the stir zone do not match the Hall–Petch relation over the entire grain size range. The experimental hardness value is higher than the value calculated by the Hall–Petch relation in the stir zone with grain size smaller than 6.4 μm. The deviation in the Hall–Petch relation was attributed to the different dislocation density and different crystallography texture strength of the sample obtained at different welding conditions.

Acknowledgements

The authors wish to acknowledge the financial support of the project “Civil Aviation Fundamental Technology Program-Advanced Materials & Process Development for Next-Generation Aircraft Structures” under the contract with RIMCOF, funded by the Ministry of Economy, Trade and Industry (METI) of Japan, a Grant-in-Aid for “Priority Assistance of the Formation of Worldwide Renowned Centers of Research – The Global COE Program (Project: Center of Excellence for Advanced Structural and Functional Materials Design)” and the Cooperative Research Project of Nationwide Joint-Use Research Institute on Development Base of Joining Technology for New Metallic Glasses and Inorganic Materials, from the Ministry of Education, Sports, Culture, Science and Technology of Japan and a Grant-in-Aid for Science Research from the Japan Society for Promotion of Science.

References

- [1] C.G. Rhodes, M.W. Ahoney, W.H. Bingel, R.A. Spurling, C.C. Bampton, *Scripta Mater.* 36 (1997) 69–75.
- [2] S. Benavides, Y. Li, L.E. Murr, D. Brown, J.C. McClure, *Scripta Mater.* 41 (1999) 809–815.
- [3] R.S. Mishra, M.W. Mahoney, S.X. McFadden, N.A. Mara, A.K. Mukherjee, *Scripta Mater.* 42 (2000) 163–168.
- [4] H.J. Liu, H. Fujii, M. Maeda, K. Nogi, *J. Mater. Proc. Technol.* 142 (2003) 692–696.
- [5] S.H.C. Park, Y.S. Sato, H. Kokawa, *Scripta Mater.* 49 (2003) 161–166.
- [6] D.Z. Zhang, M. Suzuki, K. Maruyama, *Scripta Mater.* 52 (2005) 899–903.
- [7] H.S. Park, T. Kimura, T. Murakami, Y. Nagano, K. Nakata, M. Ushio, *Mater. Sci. Eng. A* 371 (2004) 160–169.
- [8] H. Fujii, R. Ueji, Y. Takada, H. Kitahara, N. Tsuji, K. Nakata, N. Nogi, *Mater. Trans.* 47 (2006) 239–242.
- [9] W.M. Thomas, P.L. Threadgill, E.D. Nicholas, *Sci. Technol. Weld. Joining* 4 (1999) 365–372.
- [10] A.P. Reynolds, W. Tang, M. Posada, J. Deloach, *Sci. Technol. Weld. Joining* 8 (2003) 455–460.
- [11] H. Fujii, L. Cui, N. Tsuji, M. Maeda, K. Nakata, K. Nogi, *Mater. Sci. Eng. A* 429 (2006) 50–57.
- [12] R. Ueji, H. Fujii, L. Cui, A. Nishioka, K. Kunishige, K. Nogi, *Mater. Sci. Eng. A* 423 (2006) 324–330.
- [13] A.P. Reynolds, W. Tang, T. Gnaupel-Herold, H. Park, *Scripta Mater.* 48 (2003) 1289–1294.
- [14] Y.S. Sato, T.W. Nelson, C. Sterling, *Acta Mater.* 53 (2005) 637–645.
- [15] J.H. Cho, D.E. Boyee, P.R. Dawson, *Mater. Sci. Eng. A* 398 (2005) 146–163.
- [16] T. Ishikawa, H. Fujii, K. Genchi, S. Iwaki, S. Matsuoka, K. Nogi, *ISIJ Int.* 49 (2009) 897–901.
- [17] W.B. Lee, C.Y. Lee, W.S. Chang, Y.M. Yeon, S.B. Jung, *Mater. Lett.* 59 (2005) 3315–3318.
- [18] A.J. Ramirez, M.C. Juhas, *Mater. Sci. Forum* 426–432 (2003) 2999–3004.
- [19] R. John, K.V. Jata, K. Sadananda, *Int. J. Fatigue* 25 (2003) 939–948.
- [20] A.P. Reynolds, E. Hood, W. Tang, *Scripta Mater.* 52 (2005) 491–494.
- [21] S. Mironov, Y. Zhang, Y.S. Sato, H. Kokawa, *Scripta Mater.* 59 (2008) 511–514.
- [22] S. Mironov, Y.S. Sato, H. Kokawa, *Acta Mater.* 57 (2009) 4519–4528.
- [23] A.V. Sergueeva, V.V. Stolyarov, R.Z. Valiev, A.K. Mukherjee, *Scripta Mater.* 45 (2001) 747–752.
- [24] N. Kamikawa, X. Huang, N. Tsuji, N. Hansen, *Acta Mater.* 57 (2009) 4198–4208.